Available online at www.sciencedirect.com

ScienceDirect

IFAC PapersOnline CONFERENCE PAPER ARCHIVE

IFAC PapersOnLine 51-1 (2018) 371–376

Hover Corridor for a Stratospheric Airship

Gobiha D*, Nandan K Sinha**

**Ph.D. Research Scholar, Department of Aerospace Engineering (e-mail: gobiha@yahoo.com)*

***Professor, Department of Aerospace Engineering (e-mail: nandan@ae.iitm.ac.in)*

Indian Institute of Technology Madras, Chennai – 600036, India

Abstract: This paper addresses the issue of designing a feasible set of trajectories for a stratospheric airship model with the help of bifurcation based direct continuation methodology. An airship envelope is framed based on the maneuverability characteristics of the airship in the steady level circular turn maneuver. From the propounded envelope, appropriate trajectories are defined based on the application to which the airship is deployed. The proposed trajectories are then maneuvered using the nonlinear sliding mode based controller in conjunction with the three dimensional lookahead-based steering guidance law. The pertinent simulation results are presented to prove the efficacy of the designed hover corridor for the airship.

Keywords: Airship dynamics, Autonomous flight, Lighter-Than-Air vehicles, Station-Keeping.

1. INTRODUCTION

The past decade has seen a resurgence in airship technology. Being a buoyant driven vehicle, the fuel consumption of airship is frugal which paves way for eco-friendly aviation. Airships are comparatively economical and can be extensively deployed for surveillance, advertising, transportation or reconnaissance applications. All these applications either demand a straight line maneuver or a circular turn maneuver to accomplish its objective. Thus efficient and realizable maneuver design with considerations on structural, state and control constraints are of prime importance in exploiting autonomous maneuvering capabilities of the airship.

A vital prerequisite for the efficient design of control algorithm is to have an astute knowledge about the system under consideration. But most practical systems are highly nonlinear with high degrees of freedom. This makes manual or analytical analysis arduous and nearly impossible. Thus numerical analysis techniques were developed to give cognizance on the performance, trim and stability characteristics of the system. A computationally effective and robust direct continuation methodology was proposed in Vora and Sinha, 2017 using an open source MATCONT toolbox in MATLAB® environment. This tool aids the dynamical study of the nonlinear systems and it also facilitates the use of other MATLAB® subroutines in the implementation strategy.

Bifurcation and continuation methods were extensively used in literature as appraised in Paranjape et al., 2008 to perform trim and stability analysis for the highly complex aircraft models. In recent times, there has been a lot of emphasis on numerical analysis tools to assess the aircraft performance which provides strategic insights for control algorithm design. Aircraft turn performance such as maximum rate of turn was simultaneously analyzed with stability aspects in Paranjape and Ananthkrishnan, 2005. Aircraft flight and maneuvering capabilities were explored in Goman et al., 2008 by computing the attainable steady states of the system. A bound on the flight envelope based on turn and climb rate was established under faulty control surfaces (Li et al., 2012). Standard bifurcation analysis (SBA) and extended bifurcation analysis (EBA) for steady level and coordinated turn maneuvers were studied for the reviewed high altitude airship (Tiwari et al., 2016; Tiwari, 2017). But these works neither contemplate on the trajectory design aspect nor control system design to validate the proposed set of trajectories. Aircraft maneuvers were designed based on two-dimensional section of attainable equilibrium sets in Khatri et al., 2013 and nonlinear sliding mode based controller was implemented to achieve the proposed maneuver, but the trajectory design with respect to the position coordinates of the aircraft in the NED frame was not attempted which substantially curtails the practical applicability of the technique.

The novelty of this work lies in the holistic approach of operating on the inertial position coordinates to effectively design and validate the hover corridor. Parametric studies of a stratospheric airship model which were carried out using the direct continuation methodology (Tiwari et al., 2016; Tiwari, 2017) are analyzed to define a safe, practical and efficient maneuverability trajectories. The proposed trajectories are then autonomously maneuvered with the synchronous working of nonlinear sliding mode controller (SMC) and 3D guidance law.

The paper is framed in six sections. Section II briefs the modeling aspect of the stratospheric airship. Section III details the bifurcation and continuation methodology and its applicability to sketch a hover corridor for the airship. Section IV discusses the closed-loop simulation strategy to achieve the proposed trajectory. Simulated results are elaborated in section V and section VI concludes the paper.

2. STRATOSPHERIC AIRSHIP MODEL

The airship considered in this work is designed to operate in the lower stratospheric regime of the atmosphere. Such airships are called stratospheric airships and possess significant advantages over tropospheric airships. The salient features of the stratospheric airships are the lower magnitude wind speed, lack of air traffic and higher field of view. Airships also provide better resolution of images due to its closer proximity to ground compared to satellites. In addition, plaguing issues of excessive pollutant emission and big-budget

10.1016/j.ifacol.2018.05.053

are also overcome with the deployment of airships for various applications related to weather monitoring, surveillance and communication. Thus airships could be considered a potential alternative for satellites.

The equations of motion for the airship model are similar to that of aircraft, except for virtual mass and inertia terms and buoyant force of the airship. The structural and aerodynamic configurations of the evaluated airship model were carried out in Rana et al., 2015. Cruciform fin configuration has been employed at the rear end of the airship. This serves as the primary control surfaces for the airship besides providing stability to an otherwise unstable system. The four fins move in a coordinated manner to provide pitch, roll and yaw control. Based on the effect of fins on the pitch, yaw and roll motion, elevator, rudder and aileron deflections (δ_e, δ_r and δ_a) are defined to be in correspondence with the fins deflection (Rana et al., 2015).

3. SCHEMATICS OF HOVER CORRIDOR

Bifurcation based methodology has always been an attractive tool to analyze global dynamics of the system. But most of the software platforms for performing bifurcation studies were computational intensive with high dependence on the initial conditions of the system. This coupled with the model complexity greatly inhibits bifurcation analysis for airships. But the recent work of one step EBA (Vora and Sinha, 2017) substantially overcomes the computational complexity and paves way for parametric optimization design and control of airships.

Airships are capable of six degrees of freedom motion in three dimensional space. Thus, the complete dynamics of airship is captured by twelve first order nonlinear differential equations of form,

$$\dot{\boldsymbol{x}} = \boldsymbol{f}(\boldsymbol{x}, \boldsymbol{u}) \tag{1}$$

where, $\boldsymbol{x} = [V, \alpha, \beta, p, q, r, \phi, \theta, \psi, x_E, y_E, z_E] \in \mathbb{R}^{12}$ denotes the state vector and $\boldsymbol{u} = [\eta, \delta_e, \delta_a, \delta_r] \in \mathbb{R}^4$ denotes the control vector. Besides solving these set of equations simultaneously, it is also necessary to take into consideration the constraint equations. This transcribes as a precondition that there must be a minimum of n controls to satisfy n constraints. Thus, Equation 1 can be rewritten as,

$$\dot{\boldsymbol{x}} = \boldsymbol{f}(\boldsymbol{x}, s, \boldsymbol{p}) \tag{2}$$

In the above equation, $\boldsymbol{p} \in \mathbb{R}^3$ is the subset of $\boldsymbol{u}$ and it denotes the vector of control variables that is freed to achieve the proposed constraints and $s \in \mathbb{R}$ is the scalar control variable of interest and it is called continuation parameter as the dynamics of the system is characterized with respect to this parameter.

Most of the airship applications demand circular maneuvering. Thus it becomes imperative and advantageous to design a hover corridor within which the airship is safe to execute a circular turn maneuver. This is carried out by analyzing the minimum and maximum turn radius and their corresponding turn rates from the bifurcation study. The inner corridor is defined by minimum radius of turn coupled with maximum turn rate whereas the outer corridor is defined by maximum turn radius conjoined with minimum rate of turn. In order to avert turn maneuver from going haywire, a level coordinated turn is recommended. A level turn is achievable, only when the flight path angle, γ is zero. Similarly, a coordinated turn demands the bank angle, ϕ to be a constant and sideslip angle, β to be zero. But, the selection of ϕ needs a thorough perusal of the equilibrium solutions obtained in the first phase of EBA. This avoids the possibility of choosing an unachievable ϕ value. In Tiwari, 2017, ϕ is fixed at its trim value. Thus, the constraints for a level coordinated turn as contemplated in Tiwari, 2017 were given by,

$$\beta = 0; \qquad \gamma = 0; \qquad \phi = 3.54° \tag{3}$$

As it is mandatory to satisfy the three constraints specified in Equation 3, it is necessary to free three control variables. The decision on the choice of control variables to be freed is critical and could be concluded from either relative degree analysis or SBA analysis. From the bifurcation plots of SBA analysis, the control that has a significant influence on the state constraint is freed. γ is a longitudinal variable and is highly influenced by η (Tiwari et al., 2016). Thus, η is freed to satisfy the constraint on γ. Similarly, δ_a and δ_r are freed to satisfy the constraints on ϕ and β respectively (Tiwari et al., 2016). Consequently, δ_e is regarded as the continuation parameter. Thus in this case, $\boldsymbol{p} = [\eta, \delta_a, \delta_r]$ and $s = [\delta_e]$.

From the EBA analysis of the airship carried out for a level coordinated turn maneuver (Tiwari, 2017), a hover corridor is defined based on the minimum and maximum possible turn radius. The proposed envelope takes into account the stability aspect of the airship along with actuator limitation, state constraints, state bounds and structural limitations. Thus, the trajectories which are formulated to achieve specific functionalities should be in congruent with the proposed hover corridor. This assures the design of a feasible set of trajectories for the airship to be maneuvered.

4. CONTROL FORMULATION

It is necessary to validate the hover corridor that has been defined in this work. The nonlinear sliding mode based control strategy is employed in combination with the three-dimensional lookahead-based steering guidance law. This guidance law was initially proposed for the autonomous underwater vehicle (Breivik and Fossen, 2005) and later adapted for airborne vehicles (Dybsjord, 2013). Based on the proposed hover corridor, position coordinates (waypoints) are defined in the inertial frame. The guidance law generates the desired Euler angles based on the deviation between the current airship trajectory and the desired waypoints. The desired Euler angles are then post processed with the help of reference modeling and kinematic controller (Fossen, 2011) to obtain the desired body rates to be fed to the controller.

The nonlinear sliding mode based control strategy is employed to effectively achieve the desired body rates which have been generated by the guidance law. SMC framework is a robust platform to modeled and unmodeled uncertainties. Thus, SMC is considered an efficient control framework for nonlinear systems. But the variable structure framework of SMC leads to chattering phenomenon which is taken care in this work using power rate reaching law (Gao and Hung, 1993). The

equations of motion of the airship can be written in control affine form as,

$$\dot{\boldsymbol{x}} = \boldsymbol{f}(\boldsymbol{x}) + B\boldsymbol{u} \tag{4}$$

where, B denotes the input matrix. The engine thrust, η is maintained constant at the equilibrium value obtained from the bifurcation analysis. Thus, the control vector, $\boldsymbol{u} = [\delta_e, \delta_a, \delta_r] \in \mathbb{R}^3$ and it is in order with the number of states (p, q and r) to be controlled by SMC formulation. As the relative degrees of body rates p, q and r are one, sliding surface ($\mathbf{s}$) is chosen as the error (the difference between the current and the desired body rates) signal. Thus, the time derivative of the sliding surface is given by,

$$\dot{\mathbf{s}} = \boldsymbol{f}(\boldsymbol{x}) + B\boldsymbol{u} - \dot{\mathbf{d}} \tag{5}$$

where, $\mathbf{d} = [\boldsymbol{p_d}, \boldsymbol{q_d}, \boldsymbol{r_d}]$ is the reference body rates. Thus, the control vector is defined as,

$$\boldsymbol{u} = (B)^{-1}[-\boldsymbol{f}(\boldsymbol{x}) + \dot{\boldsymbol{d}} - K(\mathbf{s})sgn(\mathbf{s})] \tag{6}$$

where, $sgn(\mathbf{s})$ denotes the sign of the sliding surfaces and $K(\mathbf{s})$ is the gain matrix. $K(\mathbf{s})$ is chosen based on power rate reaching law to alleviate chattering (Gao and Hung, 1993).

$$K(\mathbf{s}) = diag(\epsilon|\boldsymbol{s}|^{\alpha}) \tag{7}$$

where, $\epsilon > 0$ and $\alpha \in (0,1)$ to provide asymptotic stability as verified in Khatri et al., 2013.

The control signals from SMC block are then fed to an actuator dynamics block which trims the control signals to satisfy saturation limitation of actuators. Limits on the elevator are chosen by analyzing the linear zone of operation of α with respect to δ_e. Similarly, limits on the aileron and rudder control surfaces are decided by considering the linear zone of operation of β with respect to δ_a and δ_r. Thus the saturation limits of the control surfaces are gauged from the bifurcation plots of δ_e vs α, δ_a vs β and δ_r vs β. From the SBA analysis of the stratospheric airship performed in Tiwari et al., 2016, limitations on the actuators are determined and the results are tabulated in Table 1.

Table 1. Constraints in actuator dynamics

Control surface	Position limits (degrees)	Rate limits (degrees/s)
Elevator	$(-25, 25)$	$(-40, 40)$
Aileron	$(-35, 35)$	$(-100, 100)$
Rudder	$(-30, 30)$	$(-82, 82)$

The control signals are eventually imparted to the airship model. The airship model provides the current states of the system. It is assumed in this work that all the states are measurable. The measured states are subsequently fed back to the guidance and the controller blocks.

5. RESULTS AND DISCUSSION

In this section, trajectories are proposed based on the designed hover corridor and its applicability in surveillance, reconnaissance and stratospheric station-keeping. The proposed trajectories are then successfully maneuvered using nonlinear SMC in conjunction with lookahead-based steering guidance law.

5.1 Surveillance and Reconnaissance Applicability

Surveillance and reconnaissance could be deemed the primary functionality of the airship. Both of these applications predominantly demand a circular turn maneuver. But the feasibility of the maneuver should be confirmed before attempting the maneuver. Bifurcation based study is explored in this work to propose a reliable trajectory. The minimum and the maximum radius of turn are computed from Tiwari, 2017 as $1200\,m$ and $58000\,m$ respectively. Thus, the proposed trajectory should lie within this corridor of $1200\,m$ and $58000\,m$ for the airship to maneuver it congenially. In this section, a trajectory of radius $12000\,m$ which falls within the bounds of the hover corridor is proposed to validate the designed airship envelope.

The proposed trajectory is then fed to the guidance framework which involves a tuning parameter called line of sight vector (R). Line of sight vector is defined as the distance between the airship and the point on the reference frame to which the airship is directed (steering point). This parameter significantly influences the maneuverability characteristics of the airship and thus the selection of R should take into account the structural, state and control constraints of the airship. Consequently, it is perceived that an optimal choice of R would be the minimum radius of turn value i.e. $1200\,m$.

The equilibrium trim conditions corresponding to a turn radius of $12000\,m$ are proposed from the bifurcation plots carried out in Tiwari, 2017. Thus, the equilibrium state vector ($\boldsymbol{x_i}$) and control vectors are given by,

$$\boldsymbol{x_i} = [11.4142, 0.0347, 0, 0, 0, 0, 0.0617, 0.0347, 0, 0, 0, -21000] \tag{8}$$

$$\eta = 0.1404, \quad \delta_e = -0.0872, \quad \delta_a = -0.3169, \quad \delta_r = 0.0987 \tag{9}$$

Based on the desired body rates computed by guidance law, SMC generates control deflections δ_e, δ_a and δ_r to achieve the proposed maneuver. Fig. 1 portrays the maneuverability of the airship for the proposed circular trajectory of radius $12000\,m$ maintained at the operational altitude of $21000\,m$. The initial position of the airship corresponds to the center of the circle and the airship makes a smooth circular maneuver along the proposed trajectory while satisfying the bounds on the state variables as assessed from Figs 2 and 3. The velocity of the airship is almost a constant at $12.4\,m/s$ throughout the maneuver (Fig. 2a). The magnitude of body axis pitch angle and pitch rate are comparatively lesser as inferred from Figs 2c and 2d. This is because of the neutral buoyancy of the airship at the operation altitude. This also explains the low magnitude of elevator deflection as concluded from Fig. 4a. The response of the sideslip angle presented in Fig. 3a shows lower magnitude oscillations around $1000\,s$. This is due to the sudden change in the maneuvering trajectory when the airship shifts from straight line maneuver to the circular maneuver. But the oscillations die down eventually and the amplitude of oscillation is not alarming. As the circular turn maneuver has higher impact on the lateral-directional dynamics, lateral-directional state variables show lower frequency fluctuations (Fig. 3). Thus lateral-directional control surfaces aileron and rudder serve a pivotal role in achieving the proposed

maneuver. Consequently, the aileron and rudder inputs are significant as depicted in Figs 4b and 4c respectively.

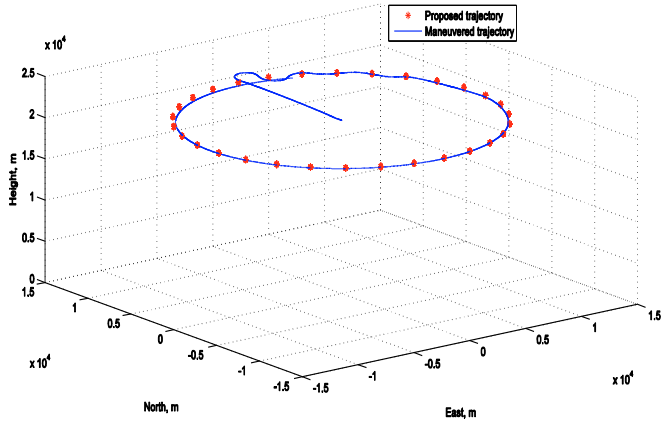

Fig. 1. Airship maneuverability for the proposed trajectory of radius, 12000 m

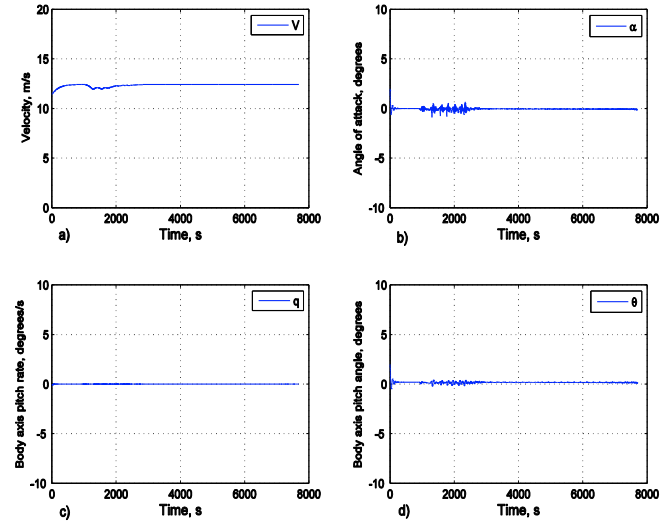

Fig. 2. Response of the longitudinal state variables for the proposed trajectory of radius, 12000 m

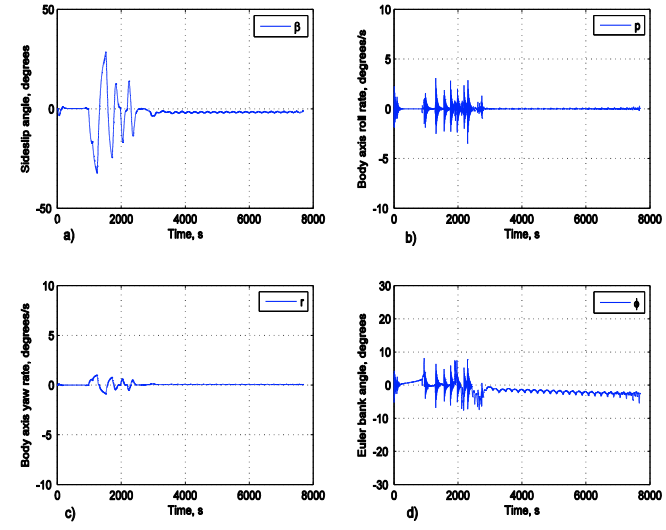

Fig. 3. Response of the lateral state variables for the proposed trajectory of radius, 12000 m

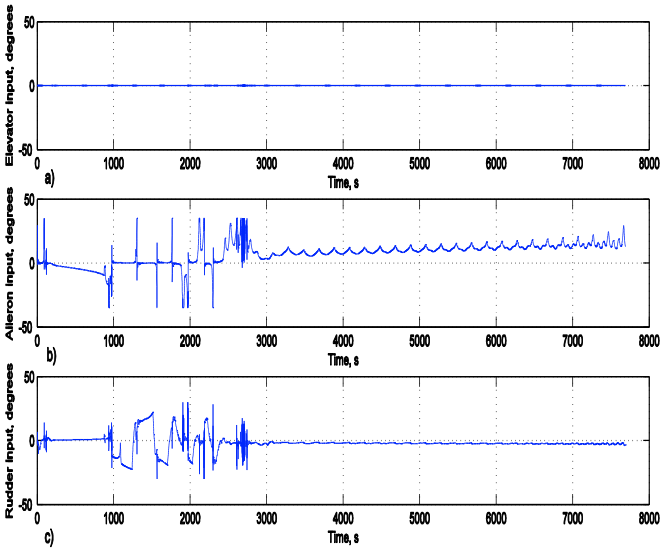

Fig. 4. Control command for the proposed trajectory of radius, 12000 m

5.2 Stratospheric Station-Keeping Applicability

Airships have a unique ability to maintain its altitude in atmosphere due to buoyancy. This makes airships a potential station-keeping platform. Geostationary satellites can operate only on the equatorial plane and it demands large expense of fuel to correct inclination changes. But stratospheric airships could be station-kept anywhere with comparatively lesser fuel. Researches on the solar powered airships are widely carried out to further improvise the fuel handling efficiency of airships (Edwards et al., 2016; Li et al., 2016). The station-keeping of airships demand significant thrust and control power due to atmospheric turbulence (Schmidt, 2007).

Station-keeping demands minimum radius turn and minimum fuel consumption. In this work, a trajectory is defined for station-keeping of airships by achieving a trade-off between these two by using the designed hover corridor. As the minimum possible turn radius is 1200 m, the airship cannot hover a circular trajectory below this radius. From the EBA for turn maneuver (Tiwari, 2017), the throttle ratio corresponding to the turn radius of 1200 m is 0.108. The maximum available engine thrust of the considered airship is 6000 N at the operational altitude of 21000 m. Thus, an engine thrust of approximately 600 N is required to carry out a circular turn of radius 1200 m. This maneuver design is more appropriate for solar-powered airships. The equilibrium state vector ($\boldsymbol{x_i}$) and control vectors are given by,

$$\boldsymbol{x_i} = [10.6178, 0.0123, 0, 0, 0, 0, 0.0617, 0.0123, 0, 0, 0, -21000] \quad (10)$$

$$\eta = 0.108, \quad \delta_e = -0.033, \quad \delta_a = -0.2632, \quad \delta_r = 0.0654 \quad (11)$$

As the proposed trajectory is a circle of radius 1200 m, the line of sight vector, R is chosen arbitrarily below this value as 900 m. The lower value of R imparts an aggressive steering as evident from Fig. 5 but the airship is station-kept in a radius of 1200 m. All state variables of the airship are within the admissible bounds (Figs 6 and 7). Though not alarming, there is a considerable offset in the sideslip angle which might be due to the structural limitation of the airship. As the radius of

turn is increased, this offset nullifies as evident from the airship maneuverability at 12000 m which is demonstrated in the previous subsection.

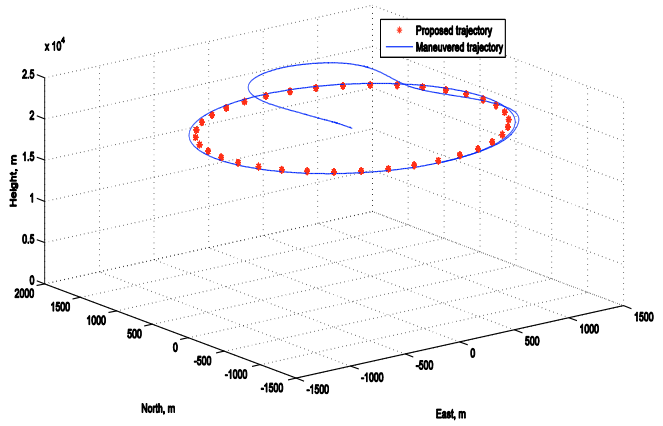

Fig. 5. Airship maneuverability for the proposed trajectory of radius, 1200 m

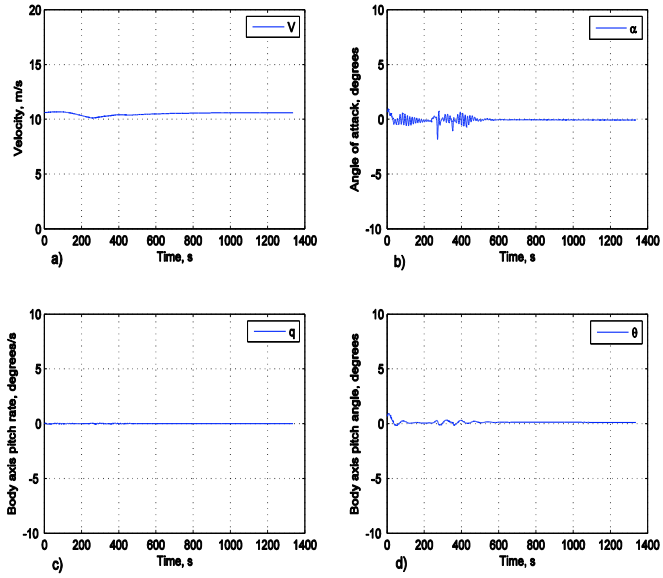

Fig. 6. Response of the longitudinal state variables for the proposed trajectory of radius, 1200 m

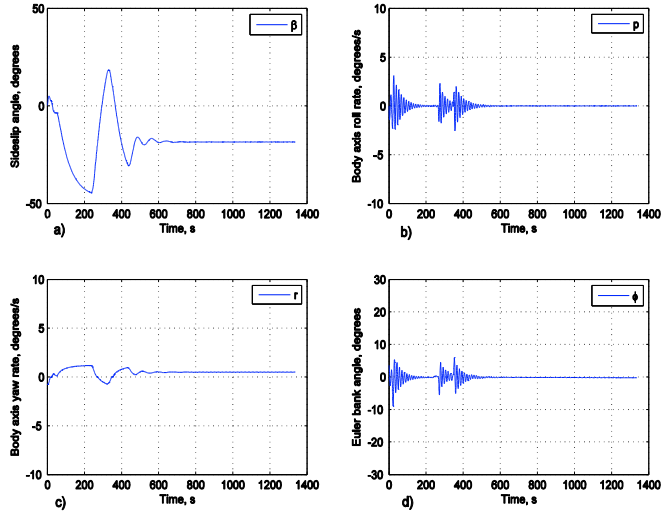

Fig. 7. Response of the lateral state variables for the proposed trajectory of radius, 1200 m

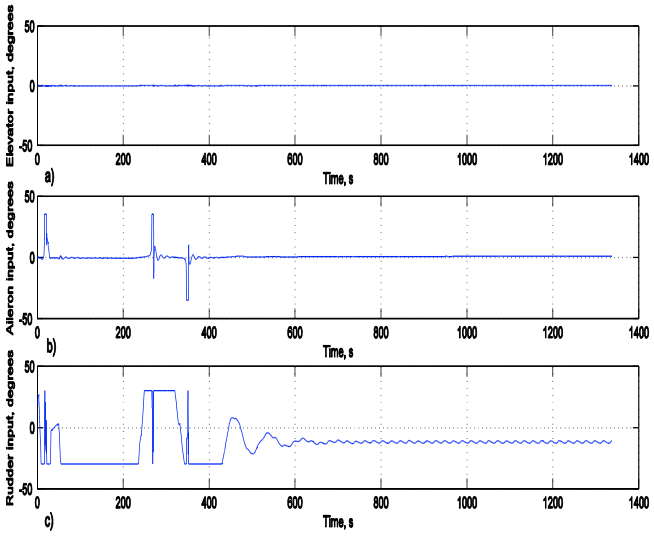

Fig. 8. Control command for the proposed trajectory of radius, 1200 m

6. CONCLUSIONS

This work proposes a novel idea of defining a toroidal shaped hover corridor for a stratospheric airship model at its operational altitude. The defined corridor takes into consideration the structural limitations, state limitations and actuator dynamics of the airship. Thus, this corridor holds enormous significance for designing reliable and workable reference trajectories for the airship to maneuver. In this work, the designed airship envelope is utilized to prescribe feasible reference trajectories for surveillance, reconnaissance and station-keeping functionalities of airship. The proposed trajectories are then congenially maneuvered with the help of nonlinear sliding mode based controller and three-dimensional guidance law. This establishes the efficacy and practicality of the designed hover corridor.

REFERENCES

Breivik, M., Fossen, T.I., (2005). Principles of guidance-based path following in 2D and 3D, *Proc. of the 44th IEEE Conference on Decision and Control, and the European Control Conf.* Seville, Spain, pp. 627–634.

Dybsjord, K.A., (2013). *Fault-Tolerant UAV Flight Control System*. M.S. dissertation, Dept. Eng. Cybernetics, NTNU, Norway.

Edwards, D.J., Kahn, A.D., Kelly, M., Heinzen, S., Scheiman, D.A., Jenkins, P.P., Walters, R., Hoheisel, R., (2016). Maximizing Net Power in Circular Turns for Solar and Autonomous Soaring Aircraft. *J. Aircr.* Vol. 53, No. 5, pp. 1–11.

Fossen, T.I., (2011). *Handbook of Marine Craft Hydrodynamics and Motion Control*, 1st ed. ed. Wiley, West Sussex, UK.

Gao, W., Hung, J.C., (1993). Variable Structure Control of Nonlinear Systems: A New Approach. *IEEE Trans. Ind. Electron.* Vol. 40, No. 1, pp. 45–55.

Goman, M.G., Khramtsovsky, A. V., Kolesnikov, E.N., (2008). Evaluation of Aircraft Performance and Maneuverability by Computation of Attainable Equilibrium Sets. *J. Guid. Control. Dyn.* Vol. 31, No. 2,

pp. 329–339.
Khatri, A.K., Singh, J., Sinha, N.K., (2013). Accessible Regions for Controlled Aircraft Maneuvering. *J. Guid. Control. Dyn.* Vol. 36, No. 6, pp. 1829–1834.
Li, J., Lv, M., Sun, K., (2016). Optimum area of solar array for stratospheric solar-powered airship. *Proc. Inst. Mech. Eng. Part G: J. Aerosp. Eng.*
Li, Y., Yang, L., Shen, G., (2012). Steady maneuver envelope evaluation for aircraft with control surface failures, *IEEE Aerospace Conference Proceedings.* Big Sky, MT, USA.
Paranjape, A.A., Ananthkrishnan, N., (2005). Airplane Level Turn Performance, Including Stability Constraints, using Extended Bifurcation and Continuation Method, *AIAA Atmospheric Flight Mechanics Conference and Exhibit.* San Francisco, California.
Paranjape, A., Sinha, N.K., Ananthkrishnan, N., (2008). Use of Bifurcation and Continuation Methods for Aircraft Trim and Stability Analysis – A State-of the-Art. *J. Aerosp. Sci. Technol.* Vol. 60, No. 2, pp. 85–100.
Rana, V., Ajith, K., Sinha, N.K., Amiatbha, P., Sati, S.C., (2015). Configuration Analysis of Stratospheric Airship, *Symposium on Applied Aerodynamics and Design of Aerospace Vehicles.* VSSC, Thiruvananthapuram, India.
Schmidt, D.K., (2007). Modeling and Near-Space Stationkeeping Control of a Large High-Altitude Airship. *J. Guid. Control. Dyn.* Vol. 30, No. 2, pp. 540–547.
Tiwari, A., (2017). *Conceptual Design and Parametric Study of High Altitude Airship Dynamics.* M.S. dissertation, Indian Institute of Technology Madras, India.
Tiwari, A., Vora, A., Sinha, N.K., (2016). Airship Trim and Stability Analysis Using Bifurcation Techniques, *7th International Conference on Mechanical and Aerospace Engineering*. London, UK, pp. 471–475.
Vora, A.S., Sinha, N.K., (2017). Direct Methodology for Constrained System Analysis with Applications to Aircraft Dynamics. *J. Aircr*.

Appendix A. EQUATIONS OF MOTION

The equations of motion of airship dynamics (Tiwari et al., 2016):

$$\dot{V} = \frac{1}{m_x}\left[T_m\eta\cos\alpha\cos\beta - \frac{1}{2}\rho V^2 S C_D - (mg - B)\sin\gamma\right]$$

$$\dot{\alpha} = q - \frac{1}{\cos\beta}\left\{\begin{array}{c}(p\cos\alpha + r\sin\alpha)\sin\beta \\ +\frac{1}{m_z V}\left[T_m\eta\sin\alpha + \frac{1}{2}\rho V^2 S C_L - (mg - B)\cos\mu\cos\gamma\right]\end{array}\right\}$$

$$\dot{\beta} = \frac{1}{m_y V}\left[\begin{array}{c}-T_m\eta\cos\alpha\sin\beta + \frac{1}{2}\rho V^2 S C_Y + \\ (mg - B)\sin\mu\cos\gamma\end{array}\right] + (p\sin\alpha - r\cos\alpha)$$

$$\dot{p} = \frac{1}{I_x}\left[\begin{array}{c}(I_y - I_z)qr + I_{xz}pq + \frac{1}{2}\rho V^2 S b C_l \\ -B b_z\sin\mu\cos\gamma\end{array}\right]$$

$$\dot{q} = \frac{1}{I_y}\left[\begin{array}{c}(I_z - I_x)pr + I_{xz}(r^2 - p^2) + \frac{1}{2}\rho V^2 S c C_m \\ +T_m\eta d_z\cos\alpha\cos\beta - B b_z\sin\gamma\end{array}\right]$$

$$\dot{r} = \frac{1}{I_z}\left[(I_x - I_y)pq - I_{xz}qr + \frac{1}{2}\rho V^2 S b C_n\right]$$

$$\dot{\phi} = p + q\sin\phi\tan\theta + r\cos\phi\tan\theta$$

$$\dot{\theta} = q\cos\phi - r\sin\phi$$

$$\dot{\psi} = \sec\theta\,(q\sin\phi + r\cos\phi)$$

$$\begin{aligned}\dot{x}_E &= V\cos\alpha\cos\beta\,(\cos\psi\cos\theta) \\ &\quad + V\sin\beta\,(\cos\psi\sin\theta\sin\phi - \sin\psi\cos\phi) \\ &\quad + V\sin\alpha\cos\beta\,(\cos\psi\sin\theta\cos\phi + \sin\psi\sin\phi)\end{aligned}$$

$$\begin{aligned}\dot{y}_E &= V\cos\alpha\cos\beta\,(\sin\psi\cos\theta) \\ &\quad + V\sin\beta\,(\sin\psi\sin\theta\sin\phi + \cos\psi\cos\phi) \\ &\quad + V\sin\alpha\cos\beta\,(\sin\psi\sin\theta\cos\phi - \cos\psi\sin\phi)\end{aligned}$$

$$\begin{aligned}\dot{z}_E &= V\cos\alpha\cos\beta\,(-\sin\theta) + V\sin\beta\,(\cos\theta\sin\phi) \\ &\quad + V\sin\alpha\cos\beta\,(\cos\theta\cos\phi)\end{aligned}$$

The wind and body axis Euler angles are in turn related by the following equations (Vora and Sinha, 2017),

$$\begin{aligned}\sin\gamma &= \cos\alpha\cos\beta\sin\theta - \sin\beta\sin\phi\cos\theta \\ &\quad - \sin\alpha\cos\beta\cos\phi\cos\theta\end{aligned}$$

$$\begin{aligned}\sin\mu\cos\gamma &= \cos\alpha\sin\beta\sin\theta + \cos\beta\sin\phi\cos\theta \\ &\quad - \sin\alpha\sin\beta\cos\phi\cos\theta\end{aligned}$$

$$\cos\mu\cos\gamma = \sin\theta\sin\alpha + \cos\alpha\cos\phi\cos\theta$$

Appendix B. NOMENCLATURE

ρ	=	density of air, kg/m^3
S	=	wing planform area, m^2
c	=	mean aerodynamic chord, m
b	=	wingspan, m
b_z	=	point of action of buoyant force along the z axis, m
d_z	=	point of action of thrust along the z axis, m
B	=	buoyant force, N
T_m	=	maximum available engine thrust, N
V	=	velocity of the airship, m/s
m	=	mass of the airship, kg
α	=	angle of attack, rad
β	=	sideslip angle, rad
p, q, r	=	body axis roll, pitch and yaw rates, rad/s
p_d, q_d, r_d	=	desired body axis roll, pitch and yaw rates, rad/s
ϕ, θ, ψ	=	Euler bank, pitch and yaw angles, rad
γ, μ	=	angles along the wind axis, rad
x_E, y_E, z_E	=	position of the airship in the inertial (NED) frame of reference, m
x_d, y_d, z_d	=	desired position of the airship in the inertial (NED) frame of reference, m
η	=	throttle ratio, available thrust to maximum thrust
$\delta_e, \delta_a, \delta_r$	=	elevator, aileron and rudder angles, rad
C_D, C_L, C_Y	=	drag, lift and side force coefficients
C_l, C_m, C_n	=	rolling, pitching and yawing moment coefficients
m_x, m_y, m_z	=	components of the apparent mass, kg
I_x, I_y, I_z, I_{xz}	=	components of the apparent moment of inertia, kg/m^2